Probe Diffusion in Intermediate Molecular Weight Polyelectrolytes: Temperature Dependence

George D. J. Phillies,*,† David Rostcheck, and Saleh Ahmed

Department of Physics, Worcester Polytechnic Institute, Worcester, Massachusetts 01609

Received February 11, 1992; Revised Manuscript Received April 2, 1992

ABSTRACT: The diffusion of 40-nm polystyrene latex spheres through solutions of two-thirds neutralized, $M_w = 5.96 \times 10^5$ poly(acrylic acid) was observed as a function of temperature T, polymer concentration c, and solution ionic strength. At fixed c, the temperature dependence of the sphere diffusion coefficient D accurately follows Walden's rule $D \sim T/\eta_s$, η_s being the *solvent* viscosity. The temperature dependence of D also follows a Vogel–Fulcher–Tamman form $T \exp(A/(T - T_0))$ closely, with a T_0 that is independent of c. Our results are consistent both with hydrodynamic scaling and with reptation/tube-type models of polymer solution dynamics but tend to reject models that ascribe the concentration dependence of D to the effect of concentration on a monomer friction coefficient or glass temperature.

Introduction

The search for a fundamental microscopic understanding of transport coefficients of nondilute polymer solutions (e.g., viscosity η, viscoelastic behavior, and self-, mutual-, and probe-diffusion coefficients [D_s, D_m, D, respectively]) is a major topic of current research. A variety of models,[1-8] each purporting to treat some or all aspects of this problem, have been propounded and debated in the literature. Whatever may be the case for polymer melts, recent reviews[9] conclude that the nature of polymer dynamics in solution remains an unsettled question.

Empirically, examinations[10-14] of a wide variety of measurements find that η, D_s, and D usually depend on concentration via a universal scaling form, namely (as written for the probe diffusion coefficient) the stretched exponential

$$D = D_0 \exp(-\alpha c^{\nu}) \tag{1}$$

Here α and ν are a scaling prefactor and exponent, respectively, while c is the polymer concentration. Experimental results supporting eq 1 include systematic measurements on systems with molecular weights up to nearly 5×10^6 [14] and concentrations approaching 300 g/L.[11] A derivation of eq 1, providing approximate numerical values for α and ν, exists in the form of a hydrodynamic scaling model.[15] In this model, which is an extension of the Kirkwood–Riseman[16] picture of interactions between pairs of polymer chains, the dominant forces are hydrodynamic, while the important motions are whole-chain translations and rotations.

One could argue that mechanisms alternative to the hydrodynamic forces invoked by ref 15 could also account for the observed near-exponential dependence of D and η on c. For example, eq 1 might arise from so-called monomer friction effects, coupled to a near-exponential dependence of the solution glass temperature T_g on c. The monomer friction coefficient ζ is the nominal quantity describing the resistance to motion experienced by a small part of a polymer chain; in the Kirkwood–Riseman model,[16] ζ is a friction factor for a single polymer bead. The monomer friction coefficient depends on polymer concentration. If c is increased, collisions between polymer chains increase ζ, thereby retarding chain diffusion and enhancing chain contributions to η.

In terms of a low-temperature glass transition, ζ depends inversely on $T - T_g$. Increasing c raises T_g toward room temperature, thereby reducing $T - T_g$ and exponentially enhancing ζ. Changes in D and η track changes in ζ, an enhancement in ζ diminishing D and increasing η. Via the action of c on T_g and ζ, increasing c thus reduces both D_s and D. By use of monomer friction effects and an appropriate relationship between c, T_g, and ζ, eq 1 may be argued to arise from a dependence of monomer subunit properties on c. If monomer friction effects were eliminated, as could be done by comparing measurements made at different c but equal $T - T_g$, the concentration dependence of D would be very different from the stretched exponential of eq 1.

The monomer friction and hydrodynamic scaling interpretations of eq 1 are opposite in nature. The monomer friction interpretation of eq 1 assigns the stretched exponential to consequences of short-range collisions between polymer beads, a bead being the smallest dynamically accessible component of a polymer chain. On the other hand, the hydrodynamic scaling model assigns eq 1 to consequences of long-range hydrodynamic forces between the largest dynamic units—translations and rotations of whole chains.

One approach to resolving the monomer friction and hydrodynamic scaling interpretations of eq 1 is to examine the temperature dependence of D and other variables. The diffusion coefficient D_1 of an isolated bead would have a temperature dependence described by the Stokes–Einstein equation

$$D_1 = k_B T/6\pi\eta_s R \tag{2}$$

where k_B is Boltzmann's constant, T is the absolute temperature, η_s is the solvent viscosity, and R is the hydrodynamic radius. Monomer friction effects depend on the distance $T - T_g$ from the glass temperature. Once the trivial dependence of D_1 on T/η_s is divided out, in the monomer friction description the temperature dependence of D arises from $T - T_g$. By measuring D as a function of c and T, one may infer T_g, allowing examination of D at various c but fixed $T - T_g$.

On the contrary, in the hydrodynamic scaling interpretation, temperature enters D primarily through its effect on the solvent viscosity. Under hydrodynamic scaling, D is predicted[15] to scale with temperature purely as T/η_s, so D/D_1 should be nearly independent of T. In some cases, T could also enter D secondarily, by changing the polymer radius of gyration; in good solvents this secondary effect should be small. (Nothing prevents monomer friction and hydrodynamic scaling effects from

† EMail: phillies@wpi.WPI.EDU.

0024-9297/92/2225-3689$03.00/0

occurring at the same time. Wheeler et al.[17,18] show an approach to removing monomer friction effects from D_s, allowing isolation of nominal hydrodynamic components of $D_s(c)$.)

We have previous reported the concentration dependence of D for probes in a variety of systems, including solutions of low[19] and intermediate[20] molecular weight poly(acrylic acids) and dextrans.[11] In each system, D showed the expected (eq 1) stretched-exponential dependence on c. This laboratory is now performing temperature studies, to separate monomer friction and hydrodynamic scaling effects in these solutions. The temperature dependence of D in low molecular weight poly(acrylic acids) was recently reported.[21] A parallel paper recently submitted for publication[22] treats $D(T)$ in dextrans.

Here we report the temperature dependence of probe diffusion in aqueous solutions of intermediate (4.5×10^5) molecular weight sodium polyacrylate (PAA). The experimental data needed to support our conclusions appear below. Supplementary figures and tables present actual lists of data points and supporting statistical analyses.

Two different approaches to characterizing $D(T)$ in systems of fixed c are employed. First, $D(T)$ will be used to infer a nominal glass temperature T_g for each solution. The starting point is the temperature dependence of η implied by the Vogel–Fulcher–Tamman equation,[23] whose form is

$$\eta = \eta_0 \exp(A/(T - T_0)) \tag{3}$$

The temperature dependence of η of many liquids is described accurately by this form, even very close to the glass. Equation 3 can be rewritten for D by applying Walden's rule $D \sim T/\eta$, to obtain

$$D = n_0 T \exp(-A/(T - T_0)) \tag{4}$$

where n_0 is a normalizing constant and T is the absolute temperature. n_0, A, and T_0 are available as fitting parameters for the nonlinear least-squares procedures applied below. The nominal glass temperature we seek to determine is approximately T_0. Redefining A via $A = \bar{A}T_0$ has no effect on how accurately either equation can describe a particular set of measurements, even though the algebraic structure of the equation is changed.

Second, hydrodynamic scaling predictions will be tested by comparing D with the generalized Stokes–Einstein form

$$D = A_0 + A_1\frac{T}{\eta_s} + A_2\left(\frac{T}{\eta_s}\right)^2 \tag{5}$$

The A_i are phenomenological coefficients determined from the data. If the orthodox Stokes–Einstein equation were followed, or if the hydrodynamic scaling predictions were correct, one would have $A_0 = A_2 = 0$. Failures of Stokes–Einstein behavior might manifest themselves as non-zero $T/\eta_s \to 0$ intercepts or as curvatures ($A_2 \neq 0$) in plots of D against T/η_s.

Experimental Methods

We used quasielastic light scattering spectroscopy (QELSS) to study the diffusion of probe particles through polymer matrices at various temperatures and polymer concentrations. Our probes were carboxylate-modified polystyrene latex spheres (PSL) of nominal diameter 38 nm (measured hydrodynamic radius of 20.4 nm). The matrix polymer was a nominal 4.5×10^5 ($M_w = 5.96 \times 10^5$) poly(acrylic acid) (PAA), two-thirds neutralized with NaOH. We employed three solvents, namely H_2O, H_2O:0.1 M NaCl, and H_2O:0.1 M NaCl:0.1 M Triton X-100 (Triton X-100: Sigma, a mixed poly(oxyethylene) surfactant). Temperatures ranged from 5 to 65 °C in increments no larger than 5 K. Computer control of the water circulator bath (Neslab) and digital autocorrelator allowed full temperature series to be obtained automatically.

Probe diffusion in PAA:H_2O was studied at polymer c of 0–3, 5, 10, 15, and 20 g/L. In 0.1 M NaCl, PAA concentrations of 0–8 g/L were employed, while in 0.1 M NaCl:0.1 wt % TX-100, PAA concentrations included 0–6, 8, and 15 g/L. The more concentrated of these solutions give a 10- or 15-fold reduction in D over its value in pure water. From our previous work[20] on probe particles in partially neutralized PAA solutions, these solutions are sufficiently concentrated to give substantially nontrivial hydrodynamic behaviors. Ionic strength effects (salt-free and 0.1 M PAA solutions are quite different) were treated in the previous paper.[20] For example, 20-nm spheres in 5 g/L PAA:0.1 M NaCl mixtures diffuse[20] 3-fold faster than expected from the measured solution viscosity and the Stokes–Einstein diffusion equation

$$D = k_B T/6\pi\eta_s R \tag{6}$$

R being the hydrodynamic radius.

Samples were prepared by filtering through 0.45-μm pore size polycarbonate membranes into disposable plastic fluorometer cells (Markson). The sample temperature was controlled to ±0.1 °C by a massive copper cell-mount through which thermostated water was passed. The sample was illuminated with a 30-mW helium–neon laser operated at the 6328-Å line. Light scattered through 90° was detected by an RCA 7265 photomultiplier tube. Typical photocount rates were $(1–3) \times 10^5$ counts/s. The signal from the photomultiplier was passed through a preamplifier–discriminator into a 144-channel Langley-Ford digital autocorrelator. Spectral integration times with 5–15 min; two or three spectra were obtained at each T.

Spectra were analyzed by the method of cumulants, in which the spectrum $S(k,t)$ is fit to

$$S(k,t) - B = [\exp(\sum_{l=0}^{N} K_l(-t)^l/l!)]^2 \tag{7}$$

Here K_l are the cumulants, N is the truncation order of the series, and the baseline B was determined experimentally by averaging the last 16 correlator channels, which are delayed 1024 channel widths from the correlator signal channels. The experimental baseline empirically is found to agree with the theoretical baseline $b = P^2/n$ (where P is the total number of counted photons and n is the total number of sample times during a measurement) to within limits consistent with the spectral signal-to-noise ratio.

The cumulants can be obtained from a weighted nonlinear least-squares fit to eq 7. Alternatively, one can write eq 7 as

$$^1/_2 \ln (S(k,t) - B) = \sum_{l=0}^{N} K_l(-t)^l/l! \tag{8}$$

Remembering that the logarithm changes the cumulant error bars, and hence the appropriate statistical weights, one can do a weighted linear least-squares fit to eq 8 and obtain the K_l. We employed the latter technique.

In sphere:PAA:water systems the spectrum is completely dominated by scattering from the spheres. For these systems the first cumulant is related to the probe diffusion coefficient D via

$$D = K_1/k^2 \tag{9}$$

where k, the magnitude of the scattering vector, is

$$k = \frac{4\pi n}{\lambda}\sin\left(\frac{\theta}{2}\right) \tag{10}$$

Here n is the index of refraction of the solvent, λ is the laser wavelength in vacuo, and θ is the scattering angle.

The second cumulant, expressed as the percent variance

$$V = 100(K_2)^{1/2}/K_1 \tag{11}$$

is a measure of the nonexponentiality of the spectrum. The spectral variance V does not enter the analysis directly but is a good indicator of sample deterioration or probe aggregation during a series of measurements. From our data, neither of these artifacts is a difficulty for the measurements reported here. V increased

Table I
Fits of Diffusion Coefficient ($10^7 D$ in Units cm²/s) to $D = n_0 T \exp(A/(T - T_0))$ with T_0 (i) Constrained to $T_0 = -124.5$ °C and (ii) Used as a Free Parameter[a]

c	n_0	A	% rmse	n_0	A	T_0	% rmse
0	0.1005	488	2.32	0.0681	373	-105	2.25
1	0.0457	530	2.40	0.0691	668	-144	2.37
2	0.0381	495	2.58	0.0370	486	-123	2.58
3	0.0258	506	1.60	0.0194	420	-111	1.57
5	0.0183	483	2.04	0.104	1184	-213	1.80
10	0.0144	480	1.66	0.0490	942	-187	1.47
15	0.00817	469	4.14	0.00535	344	-102	4.12
20	0.0107	556	3.93	0.00994	533	-121	3.92

[a] Polystyrene latex spheres (38 nm) is M_w 450 000 PAA, two-thirds neutralized, with no added salt. c is concentration in g/L; T_0 is here quoted as the Celsius temperature; and % rmse is the fractional root-mean-square error, expressed as a percentage. Percentage are reported to two places beyond the decimal to emphasize the very small improvement in fit attendant to making T_0 a free parameter.

somewhat with increasing polymer c but was usually independent of T during a given temperature series. Spectra of probes in 0.1 M NaCl or 0.1 M NaCl:0.1 wt % TX-100 systems no added PAA, showed V of 40 or 25%, respectively. Spectra in systems containing PAA but no NaCl or TX-100 were typically described adequately by a third-order cumulant fit; V was in the range 60 ± 10%. Variances were somewhat larger in solutions containing PAA and 0.1 M NaCl, but a fourth-order cumulant fit was always adequate to describe the spectra. Addition of TX-100 reduced both V and the required fit order; for PAA solutions in 0.1 M NaCl:0.1 wt % TX-100 systems, second- or sometimes third-order fits were adequate to describe spectra. In these systems, for $c < 8$ g/L, V was in the range 40 ± 5%; V increased appreciably at larger c.

The error in each fit may be characterized by the root-mean-square error

$$R = \frac{1}{M - N}\sum_{i=1}^{M}(D_i - T_i)^2 \tag{12}$$

or by the quality parameter

$$Q = \frac{1}{M - N}\sum_{i=1}^{M-1}(D_i - T_i)(D_{i+1} - T_{i+1}) \tag{13}$$

Here N is the cumulant order and M the total number of correlator signal channels. For our spectra the signal-to-noise ratio (defined as the ratio of spectral amplitude $(K_0)^2$ to the root-mean-square error R) typically ranged from 250 to 500, depending on optical alignment and sample preparation. The validity of the cumulant expansion in our signal-to-noise and variance regime has been established by extensive Monte Carlo simulations.[24]

The determination of the optimal order N for a cumulant fit to a real spectrum is an issue of some complexity. Both Q and R generally decrease with increasing fit order N. We employed four separate selection criteria to identify the best N. Every spectrum was fit to eq 8 for N of 1–4. We used the fit that exhibited a small Q (preferably $Q < 0$), a consistent fit order N for the three spectra taken of a single sample, and a small change in dQ/dN and dR/dN between the chosen N and the $N + 1$ fit and required that variances be positive.

Comparison with Vogel–Fulcher–Tamman Forms

Table I and Figures 1 and 2 present data on probes in PAA:H_2O mixtures, as described by the modified Vogel–Fulcher–Tamman equation. From Figures 1 and 2, D falls with increasing polymer concentration and decreasing T. Equation 4 manifestly provides curves that pass close to all points. Fits were made both with $T_0 = -124.5$ °C (the value obtained by fitting eq 3 to η of pure water over the temperature range we studied) and with T_0 a free parameter; the figures show the former. rms errors are in the range 1.6–4%. Freeing T_0 generally resulted in values in the region $T_0 \approx -120 \pm 20$ °C, but had virtually no effect

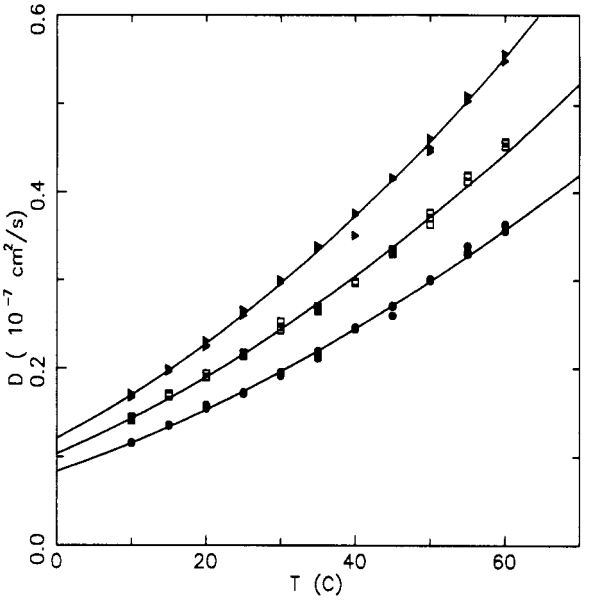

Figure 1. D (in units 1×10^{-7} cm² s⁻¹) against T for 38-nm PSL probes in PAA:H_2O mixtures at c of 3, 5, and 10 g/L. Lines represent the generalized Vogel–Fulcher–Tamman equation (eq 4) with $T_0 = -124.5$ °C.

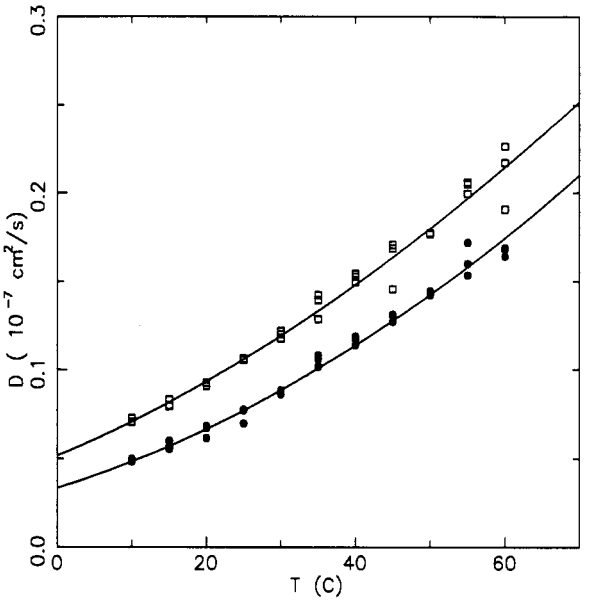

Figure 2. D (units 1×10^{-7} cm² s⁻¹) against T for 38-nm PSL probes in PAA:H_2O mixtures at c of 15 and 20 g/L. Lines represent the generalized Vogel–Fulcher–Tamman equation (eq 4) with $T_0 = -124.5$ °C.

on the quality of the fits, rms errors improving only by small fractions of a percentage point. There is no indication of an increase in T_0 with increasing c. Supplementary Tables 1–8 and supplementary Figures 1–8 list all data points and present an expanded comparison of data with fitted curves.

Table II treats the diffusion of 38-nm polystyrene latex probes through PAA:0.1 M NaCl mixtures and the description of D(T) by eq 4. The results here are qualitatively the same as results on PAA:H_2O solutions. D(T) is accurately described by a generalized VFT equation with constrained T_0 (rms errors usually 1–3%). Treating T_0 as a fitting parameter makes negligible improvements in the quality of the fit, giving best-fit T_0 values generally close to -120 °C; in a few cases, T_0 is significantly colder than -120 °C. Supplementary Tables 9–17 and supplementary Figures 9–17 give data and show in expanded form the VFT fits.

Table II
Fits of Diffusion Coefficient ($10^7 D$ in Units cm²/s) to $D = n_0 T \exp(A/(T - T_0))$[a]

c	n_0	A	% rmse	n_0	A	T_0	% rmse
0	0.0761	489	3.69	0.0731	476	−122	3.70
1	0.0638	497	1.19	0.1079	681	−152	1.15
2	0.0591	508	1.33	0.0454	427	−111	1.31
3	0.050	520	1.44	0.0491	514	−124	1.45
4	0.0399	566	1.52	0.0372	544	−121	1.52
5	0.0330	578.8	2.30	0.0847	921	−166	2.23
6	0.0309	617	1.94	0.0323	630	−126	1.95
7	0.0277	606	2.03	0.745	2122	−264	1.56
8	0.0232	626	6.87	0.0189	562	−116	6.87

[a] Polystyrene latex spheres (38 nm) in M_w 450 000 PAA, two-thirds neutralized, with 0.1 M NaCl. Other details as in Table I.

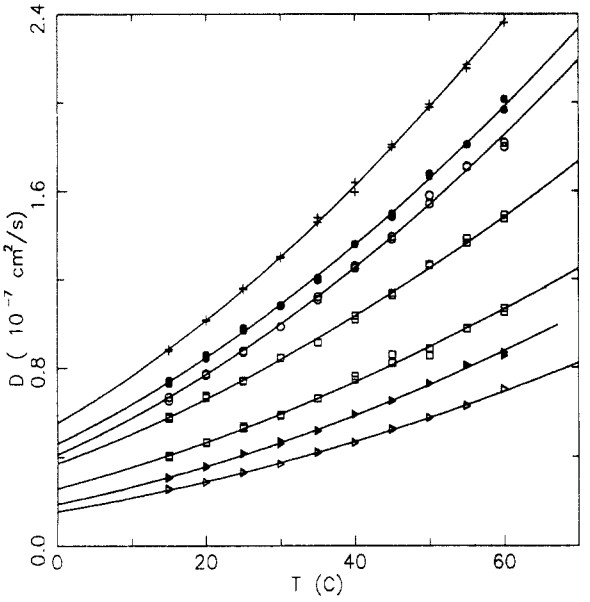

Figure 3. D (units 1×10^{-7} cm² s⁻¹) against T for 38-nm PSL probes in PAA:0.1 M NaCl:0.1 wt % TX-100 mixtures at c of 0–6 g/L. Lines show fits to eq 4 with $T_0 = -124.5$ °C.

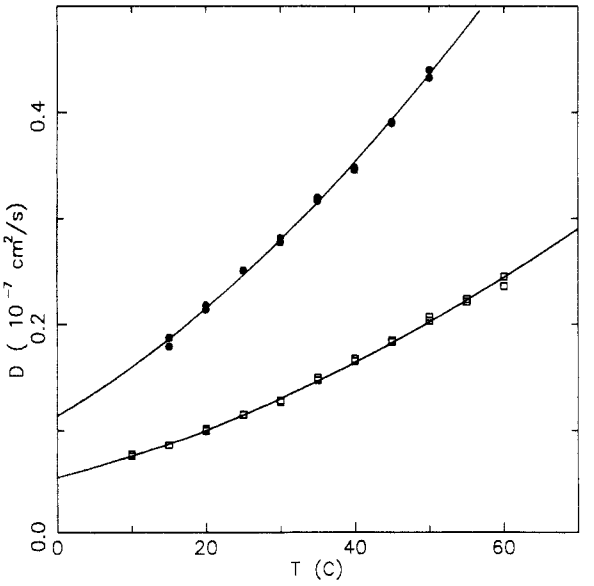

Figure 4. D (units 1×10^{-7} cm² s⁻¹) against T for 38-nm PSL probes in PAA:0.1 M NaCl:0.1 wt % TX-100 mixtures at c of 8 and 15 g/L. Curves are fits to eq 4 with $T_0 = -124.5$ °C.

Finally, Figures 3 and 4 present D of 38-nm PSL in PAA:0.1 M NaCl:0.1 wt % TX-100 systems. In all systems, eq 4 gives a good representation of $D(T)$ at all T. Table III gives fitting parameters; rms errors are 1–2% and are not appreciably improved if the constraint on T_0 is removed. Best-fit numbers for T_0 are somewhat scattered but show no indication of a trend with increasing c; indeed, the highest c values of T_0 are within 3 K of T_0 for pure water. See supplementary Tables 18–26 and supplementary Figures 18–26 for additional information.

Table III
Fits of Diffusion Coefficient ($10^7 D$ in Units cm²/s) to $D = n_0 T \exp(A/(T - T_0))$[a]

c	n_0	A	% rmse	n_0	A	T_0	% rmse
0	0.0962	481	0.74	0.0662	368	−105	0.67
1	0.0812	482	1.03	0.0788	473	−123	1.03
2	0.0835	500	2.22	0.0385	282	−85	2.09
3	0.0524	455	1.23	0.0487	691	−161	1.26
4	0.0398	466	2.05	0.0191	259	−84	1.92
5	0.0423	513	1.15	0.0276	385	−103	1.09
6	0.0311	499	0.99	0.0775	834.8	−171	0.85
8	0.0252	511	1.57	0.024	496	−122	1.57
15	0.0116	510	1.57	0.0113	500	−123	1.57

[a] Polystyrene latex spheres (38 nm) in M_w 450 000 PAA, two-thirds neutralized, with 0.1 M NaCl and 0.1 wt % TX-100 added. Other details as in Table I.

Table IV
Parameters and Ξ^2 for Fits of D to $D = A_0 + A_1(T/\eta_s)$ for 38-nm Spheres in PAA Solutions of Polymer Concentration c and the Indicated Solvent

c (g/L)		H_2O	0.1 M NaCl	0.1 M NaCl, 0.1 wt % TX-100
0	A_0	6.77×10^{-2}	3.83×10^{-3}	-1.97×10^{-2}
	A_1	3.25×10^{-2}	2.47×10^{-3}	3.53×10^{-3}
	Ξ^2	5.75×10^{-2}	5.09×10^{-4}	5.75×10^{-3}
1	A_0	-1.80×10^{-2}	1.16×10^{-2}	2.77×10^{-2}
	A_1	1.24×10^{-3}	2.01×10^{-3}	2.75×10^{-3}
	Ξ^2	4.08×10^{-3}	3.23×10^{-3}	8.52×10^{-3}
2	A_0	7.10×10^{-3}	4.70×10^{-3}	-1.23×10^{-2}
	A_1	1.22×10^{-3}	1.76×10^{-3}	2.31×10^{-3}
	Ξ^2	7.49×10^{-3}	2.21×10^{-3}	6.71×10^{-3}
3	A_0	2.03×10^{-3}	-1.65×10^{-2}	8.17×10^{-2}
	A_1	7.76×10^{-4}	1.42×10^{-3}	1.99×10^{-3}
	Ξ^2	9.52×10^{-4}	3.07×10^{-3}	2.49×10^{-3}
4	A_0		-3.46×10^{-2}	-5.59×10^{-2}
	A_1		9.16×10^{-4}	1.67×10^{-3}
	Ξ^2		6.66×10^{-4}	5.29×10^{-3}
5	A_0	7.17×10^{-3}	-3.59×10^{-3}	1.69×10^{-3}
	A_1	6.24×10^{-4}	7.21×10^{-4}	1.39×10^{-3}
	Ξ^2	1.51×10^{-3}	1.09×10^{-3}	6.47×10^{-3}
6	A_0		-3.61×10^{-2}	-4.55×10^{-2}
	A_1		5.58×10^{-4}	1.08×10^{-3}
	Ξ^2		3.74×10^{-4}	1.14×10^{-2}
7	A_0		-3.65×10^{-2}	
	A_1		5.39×10^{-4}	
	Ξ^2		5.23×10^{-4}	
8	A_0		-3.05×10^{-2}	-1.12×10^{-1}
	A_1		4.10×10^{-4}	1.06×10^{-3}
	Ξ^2		2.80×10^{-3}	3.07×10^{-2}
10	A_0	7.80×10^{-3}		
	A_1	4.95×10^{-4}		
	Ξ^2	4.66×10^{-4}		
15	A_0	8.71×10^{-3}		6.14×10^{-4}
	A_1	2.92×10^{-4}		3.42×10^{-4}
	Ξ^2	1.56×10^{-3}		1.53×10^{-4}
20	A_0	-7.04×10^{-3}		
	A_1	2.54×10^{-4}		
	Ξ^2	5.41×10^{-4}		

Probe diffusion in all systems studied—PAA:H_2O, PAA:0.1 M NaCl, and PAA:0.1 M NaCl:0.1 wt % Triton X-100—has temperature dependences which are well described by the modified Vogel–Fulcher–Tamman[23] form of eq 4. When this equation was fit to our measurements, using T_0 as a free parameter had virtually no advantage over constraining T_0 to its value for probes in pure water. We therefore find no indication that T_0 has an appreciable dependence on c or on the solution ionic strength I.

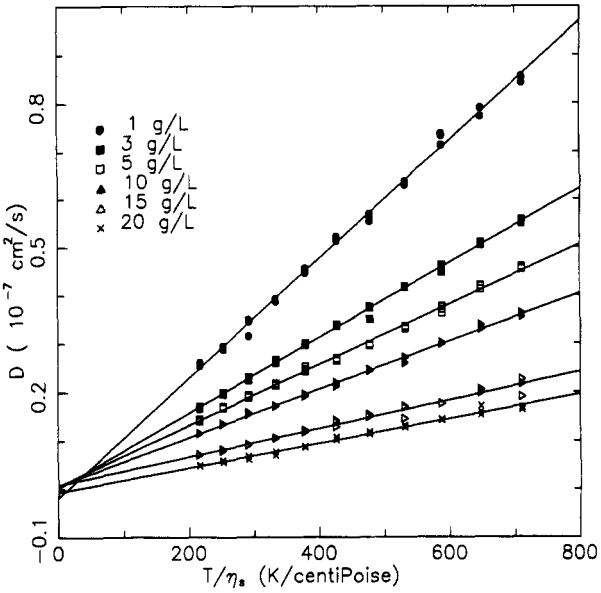

Figure 5. D (units 1×10^{-7} cm^2 s^{-1}) against T/η_s for 38 nm PSL probes in PAA:H_2O mixtures at various PAA concentrations. Curves are fits to eq 5 with $A_2 = 0$; note the very small $T/\eta_s = 0$ intercepts.

D and Solvent Viscosity η_s

To test hydrodynamic scaling and other hydrodynamic models, $D(T)$ for each polymer solution was matched via linear least-mean-squares to eq 5 while each of four sets of constraints were employed, namely (i) linear ($A_2 = 0$), (ii) forced linear ($A_0 = A_2 = 0$), (iii) quadratic (all three A_i free), and (iv) forced quadratic ($A_0 = 0$). Table IV and Figures 5–7 present the linear fits, which are the most interesting. (Complete fitting parameters for all solutions and each constraint set appear in supplementary Tables 27–29 and supplementary Figures 27–51.)

Figure 5 shows D against T/η for polystyrene sphere probes in PAA:H_2O mixtures. The scatter in the intercepts around $D = 0$ is visibly similar in size to the scatter in the data points around the best-fit lines. On comparison of different constraint sets, there is no consistent pattern of improvement of other constraint sets over the forced linear fit. In some cases the linear and forced quadratic fits are superior to the forced linear fit, in a few cases the quadratic fit is superior to the other choices. Since no systematic improvement arises from allowing A_0 or A_2 to deviate from zero, the forced linear fit ($D = A_1T/\eta_s$) is apparently appropriate for these measurements.

Figures 6 and 7 also present D as a function of T/η, for PSL in PAA:0.1 M NaCl and PAA:0.1 M NaCl:0.1 wt % TX-100 mixtures. In both figures, straight-line fits find small, scattered $T/\eta \to 0$ intercepts, whose magnitudes are similar to the scatter of individual data points around their best-fit lines. Just as was found for probes in PAA:H_2O systems, there is no systematic improvement in Ξ^2 on moving from a forced linear fit to the simple linear fit seen in the figures or to a quadratic fit. The occasional improvements seen on deconstraining one of the A_i are therefore interpreted as arising from accidental correlations in the noise. Results on the systems seen in Figures 6 and 7 are therefore consistent with the adequacy of the forced linear fit $D = A_1T/\eta_s$.

Discussion

In the above, we examined the temperature dependence of probe diffusion in two-thirds neutralized intermediate molecular weight poly(acrylic acid), comparisons being made with a Vogel–Fulcher–Tamman[23] form and

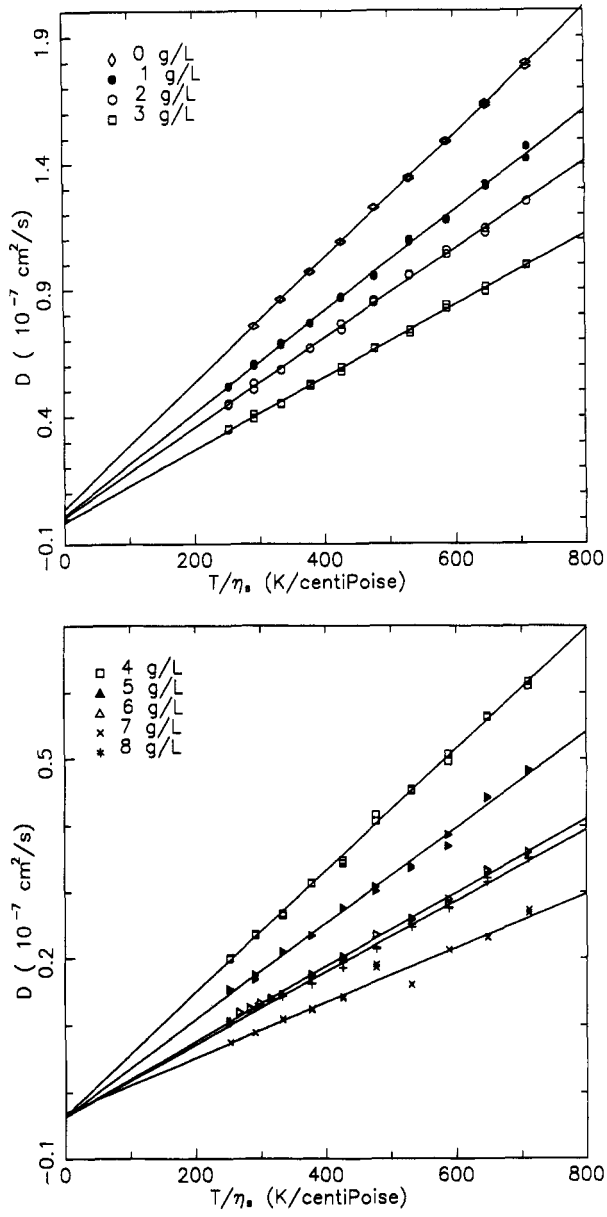

Figure 6. D (units 1×10^{-7} cm^2 s^{-1}) against T/η_s for 38-nm PSL probes in PAA:0.1 M NaCl mixtures at (a, top) low PAA concentrations and (b, bottom) more elevated PAA concentrations. Curves are fits to eq 5 with $A_2 = 0$; note the small $T/\eta_s = 0$ intercepts.

with a generalization of Walden's rule. The temperature dependence of D is almost identical with the temperature dependence of η of pure water. The observed relationships between D, η_s, and T are consistent with hydrodynamic models in which solvent-moderated hydrodynamic interactions are the dominant forces between polymer chains.[3] The same relationships are also consistent with reptation-type models for low-c solutions in which the monomer friction coefficient remains determined by the solvent viscosity.[1,2]

$D(T)$ is described well by a Vogel–Fulcher–Tamman form with a concentration-independent T_0. There is no evidence that the temperature dependence of D is modulated by a concentration dependence of glass temperature T_g or, implicitly, by a concentration dependence of the so-called monomer friction coefficient. As previously reported for solutions of low molecular weight PAA[21] and dextrans,[22] we find clear indications that the observed[29] stretched-exponential concentration dependence of D does not arise from a concentration-dependent T_g.

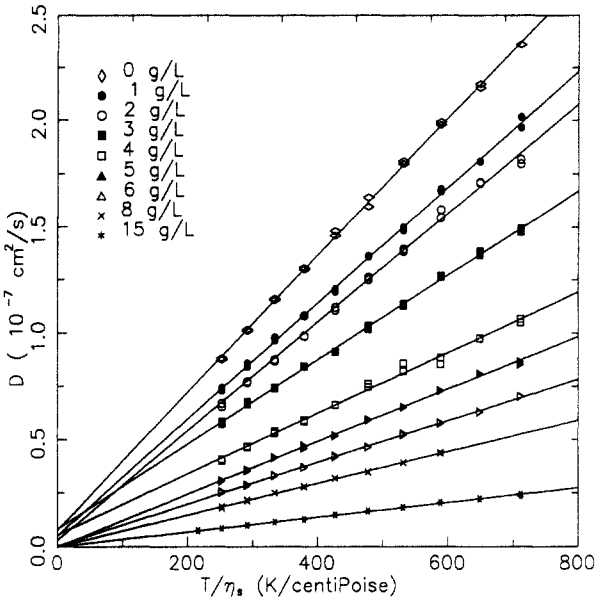

Figure 7. D (units 1×10^{-7} cm^2 s^{-1}) against T/η_s for 38-nm PSL probes in PAA:0.1 M NaCl:0.1 wt % TX-100 mixtures at various PAA concentrations. Curves are fits to eq 5 with $A_2 = 0$; note the very small $T/\eta_s = 0$ intercepts.

Supplementary Material Available: Tables of D and T/η of 38-nm sphere probes in M_w 4.5 × 10^5 PAA with H_2O, 0.1 M NaCl, and 0.1 M NaCl:0.1 wt % TX-100 and of fits of the tabulated data to $D = A_0 + A_1(T/\eta_s) + A_2(T/\eta_s)^2$ under various constraints and figures showing the tabulated data and curves representing fits to modified Vogel–Fulcher–Tamman forms and to $D = A_0 + A_1(T/\eta_s)$ (83 pages). Ordering information is given on any current masthead page.

Acknowledgment. The partial support of this work by the National Science Foundation under Grant DMR 91-15639 is gratefully acknowledged. We wish to thank Mr. Yang Xu for his technical assistance with some parts of this work.

References and Notes

(1) deGennes, P.-G. *Scaling Concepts in Polymer Physics*; Cornell University Press: Ithaca, New York, 1979, 1988.
(2) Doi, M.; Edwards, S. F. *The Theory of Polymer Dynamics*; Clarendon Press: Oxford, U.K., 1986.
(3) Phillies, G. D. J. *J. Phys. Chem.* **1989**, *93*, 5029.
(4) Hess, W. *Macromolecules* **1986**, *19*, 1395; **1988**, *21*, 2620.
(5) Oono, Y.; Baldwin, P. R. *Phys. Rev.* **1986**, *A33*, 3391.
(6) Grest, G. S.; Kremer, K. In *Springer Proceedings in Physics, Vol. 33: Computer Simulation Studies in Condensed Matter Physics*; Landau, D. P., Mon, K. K., Schuettler, H. R., Eds.; Springer-Verlag: Berlin, 1988; pp 76–83.
(7) Kolinski, A.; Skolnick, J.; Yaris, R. *J. Chem. Phys.* **1987**, *86*, 1567; **1987**, *86*, 7164; **1987**, *86*, 7174.
(8) Ngai, K. L.; Rendell, R. N.; Rajagopal, S. T. *Ann. N.Y. Acad. Sci.* **1984**, *484*, 150.
(9) Lodge, T. P.; Rotstein, N. A.; Prager, S. *Adv. Chem. Phys.* **1990**, *79*, 1.
(10) Phillies, G. D. J. *Macromolecules* **1986**, *19*, 2367.
(11) Phillies, G. D. J.; Gong, J.; Li, L.; Tau, A.; Zhang, K.; Yu, L.-P.; Rollings, J. *J. Phys. Chem.* **1989**, *93*, 6219.
(12) Phillies, G. D. J.; Peczak, P. *Macromolecules* **1988**, *21*, 214.
(13) Russo, P. S.; Mustafa, M.; Cao, T.; Stephens, L. K. *J. Colloid Interface Sci.* **1988**, *122*, 120.
(14) Zhou, P.; Brown, W. *Macromolecules* **1989**, *22*, 890.
(15) Phillies, G. D. J. *Macromolecules* **1987**, *20*, 55; **1988**, *21*, 3101.
(16) Kirkwood, J. G.; Riseman, J. *J. Chem. Phys.* **1948**, *16*, 515.
(17) Wheeler, L. W.; Lodge, T. P. *Macromolecules* **1989**, *22*, 3399.
(18) Lodge, T. P.; Markland, P.; Wheeler, L. W. *Macromolecules* **1989**, *22*, 3409.
(19) Phillies, G. D. J.; Pirnat, T.; Kiss, M.; Teasdale, N.; Maclung, D.; Inglefield, H.; Malone, C.; Yu, L.-P.; Rollings, J. *Macromolecules* **1989**, *22*, 4068.
(20) Phillies, G. D. J.; Malone, C.; Ullmann, K.; Ullmann, G. S.; Rollings, J.; Yu, L.-P. *Macromolecules* **1987**, *20*, 2280.
(21) Phillies, G. D. J.; Saleh, A.; Li, L.; Xu, Y.; Rostcheck, D.; Cobb, M.; Tanaka, T. *Macromolecules* **1991**, *24*, 5299.
(22) Phillies, G. D. J.; Quinlan, C. A. Submitted for publication.
(23) Vogel, H. *Phys. Z.* **1921**, *22*, 645. Fulcher, G. S. *J. Am. Ceram. Soc.* **1925**, *77*, 3701. Tamman, G.; Hesse, W. *Z. Anorg. Allg. Chem.* **1926**, *156*, 245.
(24) Phillies, G. D. J. *J. Chem. Phys.* **1988**, *89*, 91.

Registry No. PAA·*x*Na, 9003-04-7.